JACS
JOURNAL OF THE AMERICAN CHEMICAL SOCIETY
Communication
pubs.acs.org/JACS

Unusual Strong Incommensurate Modulation in a Tungsten-Bronze-Type Relaxor $PbBiNb_5O_{15}$

Kun Lin,[†,†] Zhengyang Zhou,[∥,†] Laijun Liu,[⊥] Hongqiang Ma,[†] Jun Chen,[†] Jinxia Deng,[†,‡] Junliang Sun,[*,∥] Li You,[§] Hidetaka Kasai,[#] Kenichi Kato,[#] Masaki Takata,[#,▽] and Xianran Xing[*,†]

[†]Department of Physical Chemistry, [‡]Department of Chemistry, and [§]State Key Laboratory for Advanced Metals and Materials, University of Science & Technology Beijing, Beijing 100083, China

[∥]College of Chemistry and Molecular Engineering, Peking University, Beijing 100871, China

[⊥]State Key Laboratory Breeding Base of Nonferrous Metals and Specific Materials Processing, Guilin University of Technology, Guilin 541004, China

[#]RIKEN SPring-8 Center, 1-1-1 Kouto, Sayo-cho, Sayo-gun, Hyogo 679-5148, Japan

[▽]Institute of Multidisciplinary Research for Advanced Materials, Tohoku University, 2-1-1 Katahira, Aoba-ku, Sendai 980-8577, Japan

Supporting Information

ABSTRACT: Pb- or Bi-based perovskite oxides have been widely studied and used because of their large ferroelectric polarization features induced by stereochemically active $6s^2$ lone pair electrons. It is intriguing whether this effect could exist in other related systems. Herein, we designed and synthesized a mixed Pb and Bi A site polar compound, $PbBiNb_5O_{15}$, with the TTB framework. The as-synthesized material turns out to be a relaxor with weak macroscopic ferroelectricity but adopts strong local polarizations. What's more, unusual five orders of incommensurate satellite reflections with strong intensities were observed under the electron diffraction, suggesting that the modulation is highly developed with large amplitudes. The structural modulation was solved with a (3 + 1)D superspace group using high-resolution synchrotron radiation combined with anomalous dispersion X-ray diffraction technique to distinguish Pb from Bi. We show that the strong modulation mainly originates from lone-pair driven Pb^{2+}−Bi^{3+} ordering in the large pentagonal caves, which can suppress the local polarization in x−y plane in long ranges. Moreover, the as-synthesized ceramics display strong relaxor ferroelectric feature with transition temperature near room temperature and moderate dielectric properties, which could be functionalized to be electromechanical device materials.

Perovskite oxides, with chemical formula of ABO_3, are well-known for their technological applications as ferroelectric and piezoelectric materials. Of particular interests are the Pb- and Bi-based ones in which the crystal structures are predistorted by the stereochemically active $6s^2$ lone pairs and many physical properties can be activated under small external stimuli.[1,2] For example, lead zirconate tianate (PZT, ca. 48% $PbTiO_3$), one of the best piezoelectrics, has excellent electromechanical properties and is extensively used as vibrators, actuators, and sensors;[3] giant polarization emerges in tetragonal-like $BiFeO_3$ thin films;[1] and multiferroics were found in $BiMO_3$, M = (Mn,[4] Fe,[5] Co,[6] $Ni_{1/2}Mn_{1/2}$,[6] etc.). Theoretical calculation suggested that B−O covalency is essential for ferroelectric instability while hybridization between Pb(Bi) 6s and O 2p states is responsible for enhanced ferroelectricity,[7] which accounts for the much larger polarization in $PbTiO_3$ compared to $BaTiO_3$. Afterward, evidence of Pb−O and Bi−O covalencies were also experimentally obtained by the MEM/Rietveld analysis against synchrotron-radiation powder diffraction data.[8]

Tetragonal tungsten bronze oxides (TTBs), the perovskite analogues, constitute the second largest class of ferroelectrics.[9] However, little attention was drawn on the lone pair A site TTBs. The TTBs are one type of nonstoichiometric compounds with a formula of $(A2)_4(A1)_2C_4B_{10}O_{30}$ (B = Nb, Ta). Similar to perovskite, their skeletons are built up by corner-sharing BO_6 octahedra, while viewing along the c-axis, these BO_6 octahedra form three different sizes of tunnels: pentagonal (A2), quadrangular (A1), and small triangular (C, usually empty and are omitted in this study) (see Figure 1), and thus, more flexibilities are included. It is anticipated that strong ferroelectric polarization may be achieved in a pure Pb or Bi A site TTB. Indeed, $PbNb_2O_6$ ($Pb_5Nb_{10}O_{30}$) was a good piezoelectric material with high ferroelectric Curie-temperature (T_C = 570 °C),[9a,10] and no pure Bi A site TTB was reported.

In this work, we designed a new TTB-type composition, $PbBiNb_5O_{15}$ ($Pb_2Bi_2Nb_{10}O_{30}$, PBN), which possesses mixed lone pair containing ions Pb and Bi in the A sites. To maintain electric neutrality, only four out of six A sites are occupied leaving the other two empty. To the best of our knowledge, it is the case that contains the most A site vacancies among the TTB niobates or tantalates (to stabilize the structure, normally more than five out of six of the A sites (A1 + A2) are occupied). The targeted compound can be synthesized and stabilized at the ambient pressure. Unlike $PbNb_2O_6$,[9a] PBN was a typical relaxor ferroelectric and the T_m, temperature at dielectric maximum, is near room temperature (RT), suggesting the low ferroelectric long-range ordering. What's more, it adopts an incommensurate modulated structure, and up to five orders of satellite reflections with strong intensities can be observed in selected area electron

Received: August 5, 2015
Published: October 16, 2015

DOI: 10.1021/jacs.5b08230
J. Am. Chem. Soc. 2015, 137, 13468−13471

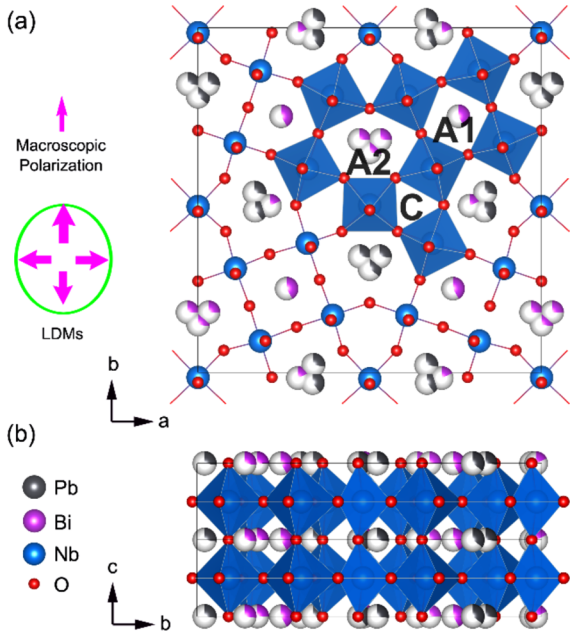

Figure 1. Average structure of PBN viewing down [001] (a) and [100] (b) directions. The color fractions of Pb (gray) or Bi (purple) atoms represent the occupancies. The atomic clusters located in the pentagonal A2 sites indicate the split positions. Only partial NbO_6 octahedra were drawn in (a) to indicate the tunnel sites. PBN adopt weak macroscopic polarization along the b_{ORT} axis, while large local dipole moments (LDMs) exist inside the $x-y$ plane (a).

diffraction (SAED) combined with multiple split A site in the pentagonal tunnels of the average structure. Such high order and high intensity satellite reflections under SAED have rarely been documented among the TTBs, suggesting that the structure may be highly modulated with large amplitudes. The modulated structure was solved in a (3 + 1)D superspace group and the positions of Pb and Bi were distinguished by anomalous dispersion X-ray diffraction. It shows that its strong modulated behavior is related to the large positional and occupational modulations induced by large local dipole moments in the A sites. In addition, the as-synthesized ceramic displays a strong relaxor behavior and moderate dielectricity, which may be used as electric materials.

Polycrystalline specimen were synthesized by solid state methods. The product was verified by powder X-ray diffraction, indicating a TTB-type structure. Rietveld analysis revealed some weak reflections that could be correlated with structural modulations. Thus, transmission electron microscope (TEM) equipped with SAED were carried out to further determine the modulation wave vectors and superspace group (Figures 2 and S1). In Figure 2, main reflections corresponding to the basic TTB cell and satellite reflections with alternatively strong and weak intensities relating to the modulation vector $\alpha(\boldsymbol{a}^* + \boldsymbol{b}^*) + \beta\boldsymbol{c}^*$ ($\alpha \approx 0.3, \beta = 0.5$) can be clearly seen (Figures 2 and S1). The orders of satellite reflections are marked by numbers in orange circles in Figure 2, and such five orders of satellite reflections with strong intensities are observed in the TTB structures for the first time, which suggests that PBN has a very strong tendency to get modulated. In addition, there is no modulation vector along $\alpha(\boldsymbol{a}^* - \boldsymbol{b}^*) + \beta\boldsymbol{c}^*$ (Figure 2b), and thus PBN is a (3 + 1)D orthorhombic TTB compounds. Then, the setting of the pseudotetragonal unit cell should be transformed into an orthorhombic cell by (110, $1\bar{1}0$, 001).[11] According to the

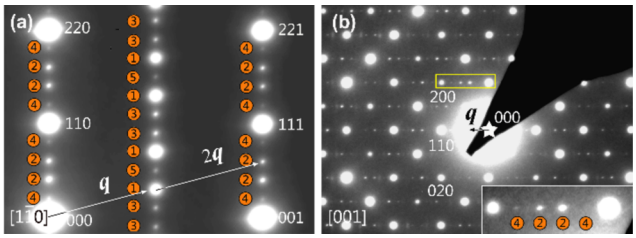

Figure 2. SAED patterns along $[1\bar{1}0]_{TTB}$ (a) and [001] (b) directions showing different orders of satellite reflections, which are positioned in both $l = 0$ and $l = 1/2$ planes (a). The numbers in the orange circles represent the orders of modulation and $\boldsymbol{q}$ is the modulation vector. The indices are labeled on the basis of basic TTB cell.

reflection conditions and thermal expansion behavior, the superspace group of PBN is determined as $Xm2m(\alpha 00)000$ (a = 17.65852(10) Å, b = 17.67709(10)Å, c = 7.75289(3) Å, α = 0.61215(4), centring vector (1/2 1/2 0 0, 0 0 1/2 1/2, 1/2 1/2 1/2 1/2)). The details of the superspace group determination are placed in the Supporting Information.

In addition to the intriguing modulation, strong frequency-dispersion were observed in the dielectric spectrum. The as-synthesized ceramic have an actual density of 5.86 g cm^{-3} measured by the Archimedes method and are 95.3(1)% of the theoretical density, revealing the ceramics were well sintered and compacted. Figure 3 shows the temperature dependence of

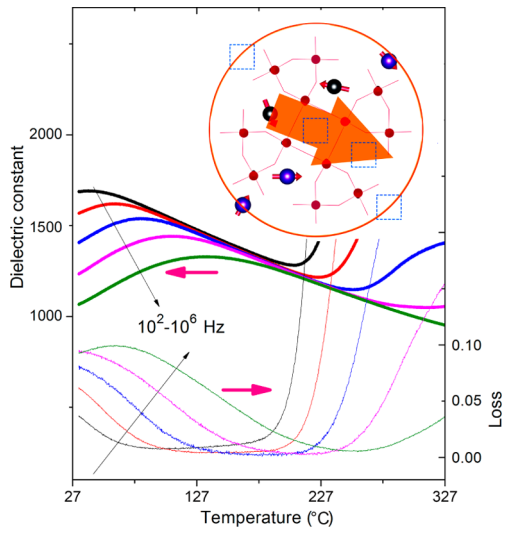

Figure 3. Temperature dependence of dielectric constant and loss above RT. Inset: Local structure of a basic TTB cell that has a large total polarization component inside the $x-y$ plane (large orange arrow), but the macroscopic polarization in the $x-y$ plane is rather small due to the incommensurate modulated long-range ordering. The small arrows represent the LDMs, and the dashed boxes indicate the vacancies in the A sites.

dielectric constant and loss measured from 30 to 327 °C at different frequencies. It shows that PBN displays an obvious relaxor behavior near RT with $T_m \approx 100$ °C (10^5 Hz), much lower than the T_C of $PbNb_2O_6$ (570 °C),[9a] $Pb_2KNb_5O_{15}$ (460 °C),[12] $PbTiO_3$ (490 °C),[13] or $BiFeO_3$ (825 °C).[14] The dielectric constant keeps a relatively stable value in a wide temperature range (30–327 °C), suggesting its potential applications, via chemical modifications, as electromechanical materials.[15,16] The dielectric data can be fitted to the modified Curie–Weiss law and Vogel–Fucher law (Figure S2),[17] and the fitted parameters are γ

DOI: 10.1021/jacs.5b08230
J. Am. Chem. Soc. 2015, 137, 13468–13471

= 1.87(1), E_a = 0.22(1) eV, T_f = 202(0) K, and f_0 = 2.03(1) × 10^{11} Hz, implying a weakly coupled relaxor feature for PBN.

To further study the exact structural feature behind relaxation and modulation, high-angular resolution synchrotron X-ray powder diffraction (SPD) experiments were conducted at BL44B2 beamline of SPring-8 equipped with a large Debye–Scherrer camera (λ = 1.08017 Å, 2θ range 7–75°).[18] The high intensities and signal-to-noise ratio allow us to refine the modulated structure successfully. However, Pb^{2+} and Bi^{3+} have similar electronic shells, and generally, the X-ray diffractions cannot distinguish them. Neither can the neutron.

Subsequently, anomalous dispersion X-ray powder diffraction (ADSPD) method was introduced to distinguish Pb from Bi.[19] The technique is based on the differences in atomic absorption edges (Figure S3). The energy of synchrotron X-ray (beamline BL02B2, SPring-8) was set to 13.01 keV (λ = 0.95276 Å), near the Pb L_{III} edge (L_{III}: Pb 13.04 keV, Bi 13.43 keV), which results in large scattering contrast between Pb and Bi but does not increase the absorptions (Table S1). The modulated structure was finally determined using two data sets simultaneously (SPD and ADSPD, Figure S4). The distributions of A-site atoms were found to be very sensitive to the calculated intensities. The resultant average structure was shown in Figure 1, where the quadrangular A1 sites are occupied by Bi only but the pentagonal A2 sites by both Pb and Bi. The details of incommensurate modulated structure analysis are placed in the Supporting Information.

What is the main factor inducing such high order and high intensity satellite reflections in SAED? The total occupancy of each A2 site is about 80(5)%, while A1 is 38(1)%. The total occupancy among A1 and A2 sites is only 2/3, leaving the rest 1/3 empty. The high vacancy rate provides more space for the A-site atoms to be relaxed to an energetically favorable state, which may promote the large modulation amplitudes. The largest occupational modulation amplitudes are 0.19(2) and 0.11(2) for Pb and Bi, respectively. What's more, the appearance of complex split atomic positions in the A2 sites suggests that the modulation is strongly dependent on the A2 atom positions. Figure 4 shows

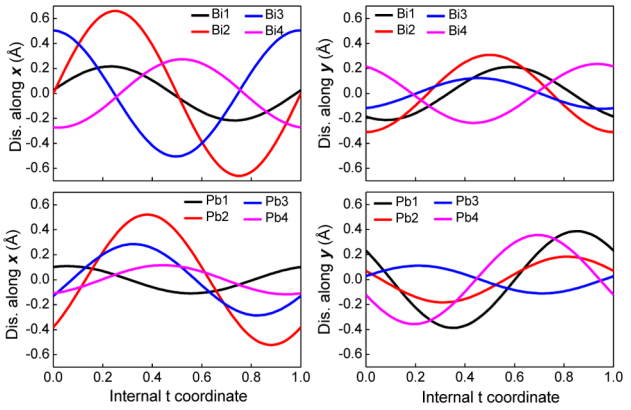

Figure 4. Deviations of the Pb and Bi atoms from their average positions as a function of the internal t coordinate.

the displacements from the average positions for Pb and Bi atoms in the internal t coordinate (see eq 1 in the Supporting Information). The largest positional displacements from average positions of the A-site cations are up to 0.52(1) and 0.66(1) Å for Pb and Bi within the x–y plane (Figure 4), much larger than other reported TTB structures.[11,20−22] In contrast, the values for $Ba_{0.39}Sr_{0.61}Nb_2O_6$[20,21] (SBN), $Ca_{0.28}Ba_{0.72}Nb_2O_6$[22] (CBN28), Ce-doped CBN28,[22] and CBN24[11] are less than 0.15 Å. In CBN28-related bronzes, the modulation amplitudes of A sites (Ba/Sr) are weak, but the displacements of their O atoms are 10 times larger than that of the A atoms,[21] implying their modulation is dominated by the configuration of NbO_6 octahedra. However, based on this study, the modulation for PBN seems to be driven and dominated by large positional and occupational deviations of A-site cations.

The most possible origin of this structural singularity in PBN belongs to the stereoactivity of $6s^2$ lone pair of Pb^{2+} and Bi^{3+} ions that have strong polarity to induce off-center displacements and form local dipole moments (LDMs).[7] To confirm the existence of the lone pairs, valence states of both Pb and Bi were investigated by Pb L_{III}-edge and Bi L_{III}-edge X-ray absorption near edge structure (XANES) spectra (see Figure S5). The absence of pre-edge peaks A and A′ indicate that the lone-pairs are not deprived from both Pb and Bi. The positions of absorption edges, energy at slope maximum, for Pb and Bi in PBN are adjacent to that of PbO and Bi_2O_3, suggesting that Pb and Bi exist in Pb^{2+} and Bi^{3+} forms. Lone pair A-site cations driven modulations were also observed in perovskites: in $Bi_2Mn_{4/3}Nb_{2/3}O_6$, incommensurate structure is produced by Bi displacement and frustrated spin order of B sites;[23] in $BiFeO_3$–$LaFeO_3$ system and Pb_2CoWO_6, by A–O antipolar displacement along with octahedral tilting.[24,25] However, these modulations are relatively weak. The strong positional and occupational modulations, as evidenced by the structural refinement and SAED in PBN, indicates its exceptional feature.

Microscopically, it is obvious that the large vacancy rates in the A sites could lead to highly inhomogeneous and uncertain of the local structure within the size of a basic TTB cell. Due to the lone pair effect, the LDMs in the A sites are large, e.g., the $Bi3O_{15}$ polyhedra are as large as −10.02/6.42/0 Debye along $x/y/z$ directions, larger than those of the $Nb1O_6$ octahedra with 0/−2.44/−0.27 Debye. Thus, as is illustrated in Figure 3 inset, large net LDMs could exert in the x–y plane of a basic TTB cell because of the A-site vacancies. However, in the long-range modulated lattice, the LDMs in the x–y plane can be canceled out. In this sense, the appearance of strong incommensurate modulation in PBN is the result of suppressing the large dipole moments in the x–y plane. This mechanism can also explain the relatively weak ferroelectric polarization evidenced by dielectric, ferroelectric, and second harmonic generation (SHG) measurements (Figure S6).

In TTB oxides, both A- and B-site disorder could induce relaxor behaviors.[26−28] The origin of relaxation is closely related to the existence of polar nanoregions (PNRs),[29] whose sizes are about 1–100 nm below "Burns" temperature. Atoms inside the PNRs should have the same lattice periodicity as the main lattice, namely, obeying long-range ordering or incommensurate modulation for PBN, but differ in relative atomic positions to generate local polarizations.[30] Thus, long-range aperiodicity and local disorder coexist, and the large positional modulation amplitudes of Pb(Bi) could partially be correlated with relaxor and dielectric responses in PBN. In the real space, the commensurately approximate unit cell is as large as 10 × $d_{(100)}$ ≈ 17.7 nm, nearly the same order to the size of PNRs.[28] The large cell dimension facilitates the formation of inhomogeneity or fluctuation of the local composition, which could contribute to relaxor behavior.

In summary, the new TTB-type compound PBN was designed and characterized, which was anticipated to be a typical

DOI: 10.1021/jacs.5b08230
J. Am. Chem. Soc. 2015, 137, 13468–13471

ferroelectric. Unexpectedly, it shows relatively weak macroscopic ferroelectric polarization but possesses strong local ones. Up to five orders of satellite reflections with strong intensities were observed along the $[110]_{TTB}$ direction under SAED, reflecting a very strong modulation. Such modulation in PBN suppresses electric dipole moments in $x-y$ plane over long-ranges that are caused by the lone-pair driven Pb−Bi ordering in the A site tunnels. The interplays between modulation, ferroelectric relaxation, and lone pair induced polarization are expected to be inspiring in investigating the underlying physics and chemistry of aperiodic materials.

■ ASSOCIATED CONTENT

Supporting Information

The Supporting Information is available free of charge on the ACS Publications website at DOI: 10.1021/jacs.5b08230.

Details of structure analysis, TEM patterns, XANES spectroscopy (PDF)
Bi1 Nb5 O15 Pb1 (CIF)

■ AUTHOR INFORMATION

Corresponding Authors

*xing@ustb.edu.cn
*junliang.sun@pku.edu.cn

Author Contributions

†Kun Lin and Zhengyang Zhou contributed equally to this work.

Notes

The authors declare no competing financial interest.

■ ACKNOWLEDGMENTS

This work was supported by National Natural Science Foundation of China (Grant Nos. 91022016, 21031005, 21231001, 91422301, 91222107), Program for Changjiang Scholars and Innovative Research Team in University (IRT1207), and the Fundamental Research Funds for the Central Universities, China (Grant No. FRF-SD-13-008A). We thank Prof. Vaclav Petricek (Institute of Physics, Academy of Sciences of Czech Republic, Czech Republic) for his useful discussion on the structural characterization.

■ REFERENCES

(1) (a) Zhang, J. X.; He, Q.; Trassin, M.; Luo, W.; Yi, D.; Rossell, M. D.; Yu, P.; You, L.; Wang, C. H.; Kuo, C. Y.; Heron, J. T.; Hu, Z.; Zeches, R. J.; Lin, H. J.; Tanaka, A.; Chen, C. T.; Tjeng, L. H.; Chu, Y. H.; Ramesh, R. *Phys. Rev. Lett.* **2011**, *107*, 147602. (b) Huang, Y. C.; Liu, Y.; Lin, Y. T.; Liu, H. J.; He, Q.; Li, J.; Chen, Y. C.; Chu, Y. H. *Adv. Mater.* **2014**, *26*, 6335.

(2) Guo, R.; Cross, L. E.; Park, S. E.; Noheda, B.; Cox, D. E.; Shirane, G. *Phys. Rev. Lett.* **2000**, *84*, 5423.

(3) Haertling, G. H. *J. Am. Ceram. Soc.* **1999**, *82*, 797.

(4) (a) Baettig, P.; Seshadri, R.; Spaldin, N. A. *J. Am. Chem. Soc.* **2007**, *129*, 9854. (b) Belik, A. A.; Iikubo, S.; Yokosawa, T.; Kodama, K.; Igawa, N.; Shamoto, S.; Azuma, M.; Takano, M.; Kimoto, K.; Matsui, Y.; Takayama-Muromachi, E. *J. Am. Chem. Soc.* **2007**, *129*, 971.

(5) Wang, J.; Neaton, J. B.; Zheng, H.; Nagarajan, V.; Ogale, S. B.; Liu, B.; Viehland, D.; Vaithyanathan, V.; Schlom, D. G.; Waghmare, U. V.; Spaldin, N. A.; Rabe, K. M.; Wuttig, M.; Ramesh, R. *Science* **2003**, *299*, 1719.

(6) Azuma, M.; Takata, K.; Saito, T.; Ishiwata, S.; Shimakawa, Y.; Takano, M. *J. Am. Chem. Soc.* **2005**, *127*, 8889.

(7) (a) Cohen, R. E. *Nature* **1992**, *358*, 136. (b) Íñiguez, J.; Vanderbilt, D.; Bellaiche, L. *Phys. Rev. B: Condens. Matter Mater. Phys.* **2003**, *67*, 224107.

(8) (a) Kuroiwa, Y.; Aoyagi, S.; Sawada, A.; Harada, J.; Nishibori, E.; Takata, M.; Sakata, M. *Phys. Rev. Lett.* **2001**, *87*, 217601. (b) Yashima, M.; Omoto, K.; Chen, J.; Kato, H.; Xing, X. *Chem. Mater.* **2011**, *23*, 3135.

(9) (a) Goodman, G. *J. Am. Ceram. Soc.* **1953**, *36*, 368. (b) Zhu, X. L.; Li, K.; Chen, X. M.; Green, D. J. *J. Am. Ceram. Soc.* **2014**, *97*, 329.

(10) Arendt, R. H.; Rosolowski, J. H. Google Patents US4234558A, 1980.

(11) Graetsch, H. A.; Pandey, C. S.; Schreuer, J.; Burianek, M.; Mühlberg, M. *Acta Crystallogr., Sect. B: Struct. Sci., Cryst. Eng. Mater.* **2014**, *70*, 743.

(12) Lin, K.; Wu, H.; Wang, F.; Rong, Y.; Chen, J.; Deng, J.; Yu, R.; Fang, L.; Huang, Q.; Xing, X. *Dalton Trans.* **2014**, *43*, 7037.

(13) Chen, J.; Hu, L.; Deng, J.; Xing, X. *Chem. Soc. Rev.* **2015**, *44*, 3522.

(14) Catalan, G.; Scott, J. F. *Adv. Mater.* **2009**, *21*, 2463.

(15) Granzow, T.; Woike, T.; Wöhlecke, M.; Imlau, M.; Kleemann, W. *Phys. Rev. Lett.* **2004**, *92*, 065701.

(16) Sun, E.; Cao, W. *Prog. Mater. Sci.* **2014**, *65*, 124.

(17) Pilgrim, S. M.; Sutherland, A. E.; Winzer, S. R. *J. Am. Ceram. Soc.* **1990**, *73*, 3122.

(18) Kato, K.; Hirose, R.; Takemoto, M.; Ha, S.; Kim, J.; Higuchi, M.; Matsuda, R.; Kitagawa, S.; Takata, M. *AIP Conf. Proc.* **2010**, *1234*, 875.

(19) Ismunandar, B. *Solid State Ionics* **1998**, *112*, 281.

(20) Woike, T.; Petříček, V.; Dušek, M.; Hansen, N. K.; Fertey, P.; Lecomte, C.; Arakcheeva, A.; Chapuis, G.; Imlau, M.; Pankrath, R. *Acta Crystallogr., Sect. B: Struct. Sci.* **2003**, *59*, 28.

(21) Surmin, A.; Fertey, P.; Schaniel, D.; Woike, T. *Acta Crystallogr., Sect. B: Struct. Sci.* **2006**, *62*, 228.

(22) Graetsch, H. A.; Pandey, C. S.; Schreuer, J.; Burianek, M.; Muhlberg, M. *Acta Crystallogr., Sect. B: Struct. Sci.* **2012**, *68*, 101.

(23) Claridge, J. B.; Hughes, H.; Bridges, C. A.; Allix, M.; Suchomel, M. R.; Niu, H.; Kuang, X.; Rosseinsky, M. J.; Bellido, N.; Grebille, D.; Perez, O.; Simon, C.; Pelloquin, D.; Blundell, S. J.; Lancaster, T.; Baker, P. J.; Pratt, F. L.; Halasyamani, P. S. *J. Am. Chem. Soc.* **2009**, *131*, 14000.

(24) Rusakov, D. A.; Abakumov, A. M.; Yamaura, K.; Belik, A. A.; Van Tendeloo, G.; Takayama-Muromachi, E. *Chem. Mater.* **2011**, *23*, 285.

(25) Baldinozzi, G.; Calvarin, G.; Sciau, P.; Grebille, D.; Suard, E. *Acta Crystallogr., Sect. B: Struct. Sci.* **2000**, *56*, 570.

(26) Arnold, D. C.; Morrison, F. D. *J. Mater. Chem.* **2009**, *19*, 6485.

(27) Zhu, X.; Fu, M.; Stennett, M. C.; Vilarinho, P. M.; Levin, I.; Randall, C. A.; Gardner, J.; Morrison, F. D.; Reaney, I. M. *Chem. Mater.* **2015**, *27*, 3250.

(28) Shvartsman, V.; Kleemann, W.; Łukasiewicz, T.; Dec, J. *Phys. Rev. B: Condens. Matter Mater. Phys.* **2008**, *77*, 054105.

(29) (a) Shvartsman, V. V.; Lupascu, D. C.; Green, D. J. *J. Am. Ceram. Soc.* **2012**, *95*, 1. (b) Shvartsman, V. V.; Dec, J.; Miga, S.; Łukasiewicz, T.; Kleemann, W. *Ferroelectrics* **2008**, *376*, 1.

(30) Xu, G.; Zhong, Z.; Bing, Y.; Ye, Z. G.; Shirane, G. *Nat. Mater.* **2006**, *5*, 134.

DOI: 10.1021/jacs.5b08230
J. Am. Chem. Soc. 2015, 137, 13468−13471